

THEORETICAL PERFORMANCE ANALYSIS OF MULTI-USER SYSTEMS WITH ONE-BIT ADCs

Phong Ngoc Dao, Hung Ngoc Dang

Posts and Telecommunications Institute of Technology

Tóm tắt—This paper investigates the theoretical performance of multi-user systems using One-bit analog-to-digital converters (ADCs). Through simulations with varying user configurations (10, 40 and 200 users), we observe that the uplink sum rate increases significantly for smaller user groups but tends to stabilize as the number of users grows due to multi-user interference. As the number of base station antennas increases, the system's capacity to handle more users improves, but the sum rate improvement slows down at higher user densities. These results provide valuable insights for optimizing system design in Multi-User systems with One-bit ADCs, highlighting that finding the right balance between user count and antenna numbers is essential for achieving optimal uplink sum-rate performance.

Từ khóa—Multi-User System, One-bit ADC, Uplink Achievable Rate

I. INTRODUCTION

In upcoming wireless networks like 5G and beyond, Multi-User systems equipped with hundreds of antennas are key to boosting spectral efficiency, improving reliability, and reducing power usage [1], [2]. However, the large number of antennas also brings significant challenges in both RF and baseband signal processing [3], [4]. A major issue is the high cost and power consumption of ADCs and digital-to-analog converters (DACs), which grow exponentially as the resolution of these converters increases. To address this issue, low-resolution ADCs, such as 1-bit or 2-bit converters, have been proposed as an effective solution to significantly cut down power consumption and reduce hardware costs [5], [6], [7], [8].

As the shift toward 5G and anticipated 6G networks drives demand for high spectral efficiency, low-resolution ADCs play a pivotal role in enabling Multi-User Systems to meet performance and energy constraints at scale [9], [10]. Traditional high-resolution ADCs introduce computational complexity and power consumption challenges that grow nonlinearly with each additional bit of resolution, which is particularly problematic in scenarios with large antenna arrays. Low-resolution ADCs, by contrast, offer a practical trade-off, enabling feasible implementations while

meeting reasonable performance standards in multi-user environments [10], [11].

Systems with low-resolution ADCs have been thoroughly analyzed from a theoretical perspective. Although low-resolution ADCs introduce quantization errors and affect the accuracy of channel estimation, Xu et al. have shown that the addition of more receive antennas helps to offset these issues, thereby maintaining overall system performance [12]. A study by Fan et al. [3] showed that increasing the number of antennas could simultaneously reduce the degradation resulting from ADC quantization and keep it energy efficient. Others include learning-based methods [13] and mixed-resolution ADC configurations [8] for further performance improvement of the system, particularly in challenging environments where there is no or limited CSI. It gives some promising directions that can be helpful for making low-resolution ADC systems useful in real deployment.

In previous research, we optimized the quantization distortion of uniform scalar quantizers to improve the achievable sum rate in multi-user systems utilizing low-resolution ADCs, with a particular focus on 1-bit ADCs [14]. In this paper, we build upon that work by solely examining the uplink sum rate across different user counts and base station antenna configurations. Our goal is to provide a more comprehensive understanding of how low-resolution ADCs affect uplink performance and to identify optimal setups that maximize the sum rate in multi-user environments.

II. SYSTEM MODEL

Consider an uplink communication scenario where M users, each equipped with a single antenna, transmit signals to a base station (BS) equipped with N antennas. This configuration is commonly referred to as a multi-user multiple-input multiple-output system, as illustrated in Fig. 1. In this model, each user transmits a symbol through a shared channel matrix \mathbf{G} , which characterizes the propagation conditions between each user and each antenna at the BS. The channel model for MU-Multi-User systems is described as follows:

$$\mathbf{y} = \sqrt{p_u} \mathbf{G} \mathbf{s} + \mathbf{n} \quad (1)$$

Contact author: Hung Ngoc Dang,

Email: hungdn@ptit.edu.vn

Manuscript received: 10/2024, revised: 11/2024, accepted: 12/2024

where $\mathbf{G} \in \mathbb{C}^{N \times M}$ represents the channel matrix between the users and the BS, \mathbf{s} is the $M \times 1$ vector containing the symbols transmitted by the users, and $\mathbf{n} \sim \mathcal{CN}(0, \mathbf{I})$ is the complex Gaussian noise vector with zero mean and unit variance. The received signal vector, $\mathbf{y} \in \mathbb{C}^{N \times 1}$, aggregates the transmitted symbols and is affected by channel and noise conditions, across the BS antennas.

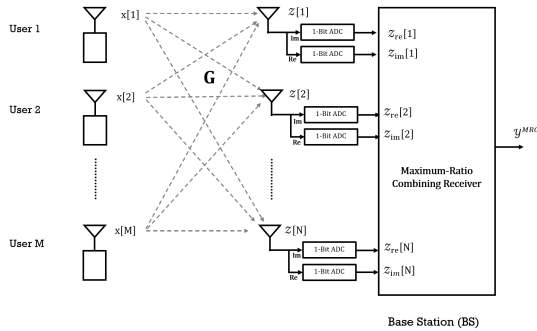
Each entry of \mathbf{G} , denoted as $g[n, m]$, models the combined effects of fast-fading and large-scale fading, where $g[n, m]$ represents the path gain from the m^{th} user to the n^{th} antenna at the BS. Specifically, $g[n, m]$ includes both the fast-fading gain, $h[n, m]$, and large-scale effects, modeled by $\phi[m]$, which capture path loss and shadow fading. The fast-fading component, $h[n, m]$, varies with user mobility and surrounding environment, while $\phi[m]$ is assumed constant over the BS antenna array [3]. The channel coefficient $h[n, m]$ can be expressed as

$$g[n, m] = h[n, m] \sqrt{\phi[m]}, \quad (2)$$

where $h[n, m]$ represents the fast-fading gain from the m^{th} user to the n^{th} antenna at the BS, and $\phi[m]$ accounts for both geometric attenuation and shadow fading, assumed to be constant across the antenna array [3]. In matrix notation, this relationship is written as

$$\mathbf{G} = \mathbf{H}\Phi^{1/2}, \quad (3)$$

where \mathbf{H} is the $N \times M$ fast-fading matrix between the users and the BS, and Φ is an $M \times M$ diagonal matrix with diagonal entries $\phi[m]$.



Hình 1. Multi-User MIMO One-bit ADC Channel Model.

Upon receiving the signal, each BS antenna processes it using a pair of one-bit ADCs. These ADCs operate separately on the in-phase (real) and quadrature (imaginary) components of the received signal, represented by \mathbf{z}_{re} and \mathbf{z}_{im} , respectively. Denote the quantization operation by \mathcal{Q} . The relationship between the input and output of the one-bit ADC block is expressed as

$$\mathbf{y} = \mathcal{Q}(\mathbf{z}_{re}) + j\mathcal{Q}(\mathbf{z}_{im}), \quad (4)$$

where \mathbf{z}_{re} and \mathbf{z}_{im} are the real and imaginary parts of the received signal \mathbf{z} , respectively. The quantizer \mathcal{Q} operates independently on each component, converting them to discrete levels that capture the primary signal characteristics while introducing quantization noise.

In this work, we use the additive quantization noise model (AQNM) for Multi-User systems with low-resolution ADCs [15], where the quantization noise as an additive distortion to the original signal. This model allows us to account for quantization effects without significantly complicating system analysis, as it approximates the quantization noise as Gaussian noise, whose variance depends on the signal power and quantizer resolution. The relationship between the input and output of the quantizer, as described in (4), can be expressed as [3]

$$\mathbf{y} = \varphi \mathbf{z} + \mathcal{W}_Q, \quad (5)$$

where $\varphi = 1 - \kappa$ represents the performance efficiency of the quantizer, κ is the inverse of the signal-to-quantization-distortion ratio (SQDR), and \mathcal{W}_Q denotes the additive quantization noise. Here, κ plays a critical role in determining the quantization efficiency, as it directly influences the amount of distortion introduced by the quantizer. By minimizing κ , the performance metric φ improves, yielding a more accurate representation of the received signal, even under the constraints of low-resolution ADCs.

Finally, the quantized signal vector is processed using maximum-ratio combining (MRC). This technique maximizes the signal-to-noise ratio (SNR) by coherently combining signals received across different antennas, thus enhancing the system's robustness against noise and interference. The combined signal \mathbf{y}^{MRC} can be expressed as

$$\mathbf{y}^{MRC} = \mathbf{G}^H \mathbf{y}, \quad (6)$$

where \mathbf{G}^H is the conjugate transpose of the channel matrix \mathbf{G} . The sum-rate approximation for the MU-MIMO channel is given by [3]

$$\mathbf{R} = \sum_{m=1}^M \log_2 \left(1 + \frac{p_u \varphi \mathcal{I}_m (N+1)}{\mathcal{I}_m} \right), \quad (7)$$

where the term $p_u \varphi \mathcal{I}_m (N+1)$ represents the received power of the m^{th} user across the N antennas at the BS. This term is directly proportional to φ , which measures the performance quality of the quantizer—the higher the value of φ , the better the quantizer performs. On the other hand, the term \mathcal{I}_m in (7), as defined in (8), is a composite measure of inter-user interference, quantization noise, and additive white Gaussian noise.

$$\mathcal{I}_m = p_u \varphi \sum_{i=1, i \neq m}^M \phi_i + p_u (1 - \varphi) \left(\sum_{i=1}^M \phi_i + \mathcal{I}_m \right) + 1. \quad (8)$$

In terms of quantization distortion, a higher value of φ directly results in a reduction of the interference term, \mathcal{I}_m . This implies that improving the quantizer's performance metric, φ , will lead to an increase in the achievable uplink sum-rate for any given ADC resolution.

Building on previous research focused on optimizing uniform quantizers for 1-bit ADC systems, this paper adopts the optimized uniform quantizer discussed earlier, which has shown significant performance improvements, especially for low-resolution ADCs like the 1-bit ADC [14], [11]. The selection of optimal truncation limits for uniform scalar quantizers is crucial, as these limits balance the overload and granular distortion in low-resolution quantization, achieving higher accuracy and enhanced performance merit φ . The optimal truncation limits for uniform scalar quantizers were carefully chosen to balance overload and granular distortion, resulting in an optimized performance merit φ . The optimized uniform quantizer dramatically improves the performance of 1-bit ADC systems, achieving a performance merit $\varphi = 0.6261$, compared to the 0.1371 value of the conventional three-sigma quantizer [14]. Such improvement in φ contributes directly to increased sum-rate performance, especially in systems where low-resolution ADCs are deployed to conserve energy. This improvement leads to a higher uplink sum-rate, making the optimized quantizer crucial for Multi-User systems with low-resolution ADCs. While the performance gap between the two quantizers narrows at higher resolutions, 1-bit and 2-bit ADCs remain the most energy-efficient.

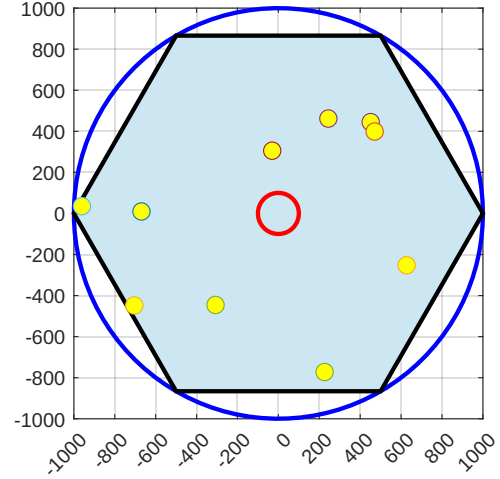
With these findings, we now turn our attention to the experimental evaluation, focusing on uplink sum-rate across various numbers of users at base station configurations for 1-bit optimized ADCs in Multi-User systems.

III. SIMULATIONS AND RESULTS

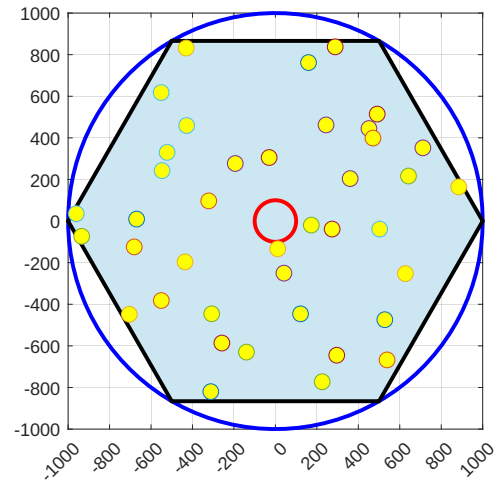
We perform simulations to analyze the uplink sum-rate for a hexagonal cell with a radius of $R = 1000$ meters. M users are randomly placed within the cell using a uniform distribution, excluding a central zone with a radius of $r_c = 100$ meters. This exclusion zone simulates realistic base station placement where users are not located directly adjacent to the antenna array [3], [16]. In this simulation, we vary the number of users, setting $M = 10, 40$ and 200 to assess the uplink sum-rate performance across different user densities. Each user count is a subset of the next; specifically, the placement of 10 users is retained within the setup for 40 users, and likewise, all 40 users are retained within the setup for 200 users. This cumulative user placement approach allows for a consistent basis of comparison across different densities, as the same initial 10 and

40 users remain in their positions within the 200 users scenario.

This layering of user groups provides insight into how additional users contribute to interference and impact sum-rate performance under the same base layout. The details of user position distribution for all setting M are illustrated in Fig. 2,3,4, respectively.



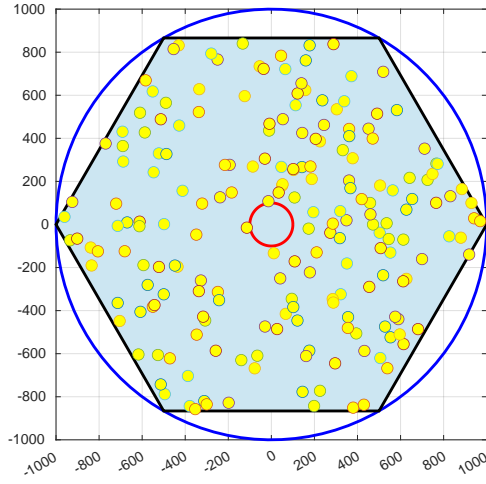
Hình 2. User placement for 10 users in the cell.



Hình 3. User placement for 40 users in the cell.

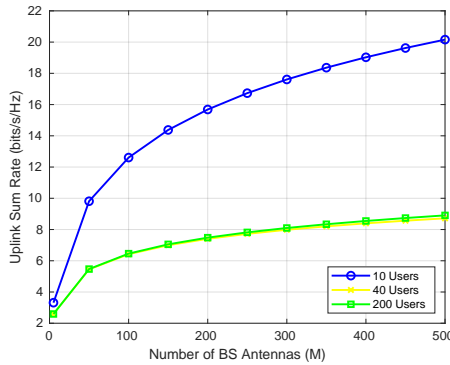
As described above, the simulations utilize 1-bit ADCs for signal quantization, simulating scenarios that prioritize energy efficiency. The use of low-resolution ADCs introduces quantization noise, modeled using the additive quantization noise model (AQNM), which treats quantization noise as an additive distortion based on signal power and ADCs resolution. The large-scale fading component \mathcal{I}_m in (8) is modeled using a log-normal distribution as follows:

$$\mathcal{I}_m = z_m \times \left(\frac{r_m}{r_c} \right)^{-\nu} \quad (9)$$



Hình 4. User placement for 200 users in the cell.

where r_m is the distance from the m^{th} user to the BS, ν is the path loss exponent, and z_m represents the log-normal random variable with a standard deviation of σ_s . Same with the assumption made in [3], we assume that the large-scale fading coefficient \mathcal{I}_m as constant once the m^{th} user is placed within the cell. For all the simulation, we assume $\sigma_s = 8$ dB and path loss exponent $\nu = 3.8$.



Hình 5. Uplink Sum-Rate for Various Numbers of Users

The results of the uplink sum-rate simulation are presented in Fig. 5. At smaller users, $M = 10$, the uplink sum-rate sees a significant boost as the number of base station antennas (M) increases, benefiting from the spatial diversity and improved signal-to-noise ratio (SNR) provided by multiple antennas. This significant boost reflects the system's ability to leverage each additional antenna to improve the spatial separation of signals, reducing interference and enhancing overall data throughput. However, As the user count increases to $M = 40$ and $M = 200$, the improvement in sum-rate slows down and eventually levels off. Importantly, $M = 200$, there is little to no improvement beyond 40 base station antennas, resulting in almost flat curves. This leveling off indicates that, at higher user densities,

the system reaches a saturation point where adding more antennas no longer significantly enhances the sum-rate.

This behavior can be explained by the inherent limitations imposed by multi-user interference. With fewer users, each user benefits significantly from the spatial diversity and beamforming advantages that come with an increased number of antennas, which help to isolate and amplify individual user signals. In this low-density scenario, the base station can spatially separate users more effectively, making it possible to achieve higher sum-rates as the number of antennas increases.

In contrast, for larger users, the base station's spatial multiplexing capability becomes a limiting factor. As the number of users exceeds the number of spatial paths that can be distinctly resolved by the base station, multi-user interference grows. This interference effectively reduces the marginal gain in sum-rate achieved by adding more antennas, as the base station struggles to spatially isolate all users simultaneously. The uplink sum-rate thus reaches a threshold, beyond which further increases in the number of antennas yield negligible improvements due to the inability to overcome the multi-user interference.

This phenomenon highlights a critical design trade-off in multi-user systems with one-bit ADCs. While one-bit ADCs provide a low-cost, energy-efficient solution, their limited resolution increases the impact of multi-user interference in high-density scenarios. The decrease in performance as the number of users increases underscores the spatial resource limitations when serving a large number of users, particularly when using low-resolution ADCs. Therefore, in high-density environments, alternative strategies, such as mixed-ADC architectures, may be necessary to maintain desirable sum-rate performance.

IV. CONCLUSIONS

In this study, we investigated the theoretical performance of Multi-User systems using One-bit ADCs. Our simulations results showed that with smaller user ($M = 10$), significant improvements in the uplink sum-rate can be achieved as the number of base station antennas increases. However, as the user grows to 40 and 200, the sum-rate begins to level off, particularly beyond 40 base station antennas, due to the increasing impact of multi-user interference. This underscores the complex of system design when deploying Multi-User systems with low-resolution ADCs, especially One-bit ADC. Further researchs will be essential to explore how the system balances performance with energy efficiency, as understanding the trade-offs between sum-rate and power consumption will be critical for optimizing future Multi-User systems using One-bit ADCs.

TÀI LIỆU THAM KHẢO

- [1] K. B. Letaief, W. Chen, Y. Shi, J. Zhang, and Y. A. Zhang, "The roadmap to 6G: AI empowered wireless networks," *IEEE Communications Magazine*, vol. 57, no. 8, pp. 84–90, Aug. 2019.
- [2] Z. Zhang, Y. Xiao, Z. Ma, M. Xiao, Z. Ding, X. Lei, G. K. Karagiannidis, and P. Fan, "6G wireless networks: Vision, requirements, architecture, and key technologies," *IEEE Vehicular Technology Magazine*, vol. 14, no. 3, pp. 28–41, Sep. 2019.
- [3] L. Fan, S. Jin, C. Wen, and H. Zhang, "Uplink achievable rate for massive mimo systems with low-resolution ADC," *IEEE Communications Letters*, vol. 19, no. 12, pp. 2186–2189, Dec 2015.
- [4] W. Fukuda, T. Abiko, T. Nishimura, T. Ohgane, Y. Ogawa, Y. Ohwatari, and Y. Kishiyama, "Low-complexity detection based on belief propagation in a massive MIMO system," in *Proc. IEEE Vehicular Technology Conference (VTC)*, June 2013, pp. 1–5.
- [5] C. Zhang, Y. Jing, Y. Huang, and X. You, "Massive MIMO with ternary ADCs," *IEEE Signal Processing Letters*, p. 1, 2020.
- [6] T. Liu, J. Tong, Q. Guo, J. Xi, Y. Yu, and Z. Xiao, "Energy efficiency of massive MIMO systems with low-resolution adcs and successive interference cancellation," *IEEE Transactions on Wireless Communications*, vol. 18, no. 8, pp. 3987–4002, Aug. 2019.
- [7] J. Dai, J. Liu, J. Wang, J. Zhao, C. Cheng, and J. Wang, "Achievable rates for full-duplex massive MIMO systems with low-resolution ADCs/DACs," *IEEE Access*, vol. 7, pp. 24 343–24 353, 2019.
- [8] L. V. Nguyen, D. T. Ngo, N. H. Tran, A. L. Swindlehurst, and D. H. N. Nguyen, "Supervised and semi-supervised learning for MIMO blind detection with low-resolution ADCs," *IEEE Transactions on Wireless Communications*, p. 1, 2020.
- [9] X. Hu, C. Zhong, X. Chen, W. Xu, H. Lin, and Z. Zhang, "Cell-free massive mimo systems with low resolution adcs," *IEEE Transactions on Communications*, vol. 67, no. 10, pp. 6844–6857, 2019.
- [10] J. Zhang, J. Zhang, and B. Ai, "Cell-free massive mimo with low-resolution adcs over spatially correlated channels," in *ICC 2020 - 2020 IEEE International Conference on Communications (ICC)*, 2020, pp. 1–7.
- [11] J. Zhang, L. Dai, S. Sun, and Z. Wang, "On the spectral efficiency of massive mimo systems with low-resolution adcs," *IEEE Communications Letters*, vol. 20, no. 5, p. 842–845, May 2016. [Online]. Available: <http://dx.doi.org/10.1109/LCOMM.2016.2535132>
- [12] L. Xu, X. Lu, S. Jin, F. Gao, and Y. Zhu, "On the uplink achievable rate of massive MIMO system with low-resolution ADC and RF impairments," *IEEE Communications Letters*, vol. 23, no. 3, pp. 502–505, Mar. 2019.
- [13] S. Gao, P. Dong, Z. Pan, and G. Y. Li, "Deep learning based channel estimation for massive MIMO with mixed-resolution ADCs," *IEEE Communications Letters*, vol. 23, no. 11, pp. 1989–1993, Nov. 2019.
- [14] H. N. Dang, T. V. Nguyen, and H. T. Nguyen, "Improve uplink achievable rate for massive mimo systems with low-resolution adcs," in *2020 IEEE Eighth International Conference on Communications and Electronics (ICCE)*, 2021, pp. 99–104.
- [15] M. Srinivasan and S. Kalyani, "Analysis of massive MIMO with low-resolution ADC in nakagami- m fading," *IEEE Communications Letters*, vol. 23, no. 4, pp. 764–767, Apr. 2019.
- [16] H. Q. Ngo, E. G. Larsson, and T. L. Marzetta, "Energy and spectral efficiency of very large multiuser MIMO systems," *IEEE Transactions on Communications*, vol. 61, no. 4, pp. 1436–1449, Apr. 2013.

PHÂN TÍCH HIỆU SUẤT LÝ THUYẾT CỦA HỆ THỐNG ĐA NGƯỜI DÙNG VỚI BỘ ADC MỘT BIT

Tóm tắt - Bài báo này nghiên cứu hiệu suất lý thuyết của các hệ thống đa người dùng sử dụng bộ chuyển đổi tương tự sang số (ADC) một bit. Thông qua các mô phỏng với các cấu hình người dùng khác nhau 10, 40 và 200 người, chúng tôi quan sát thấy rằng tổng tốc độ truyền lên tăng đáng kể khi số lượng người dùng nhỏ nhưng có xu hướng ổn định khi số lượng người dùng tăng lên do ảnh hưởng của nhiễu đa người dùng. Khi số lượng ăng-ten tại trạm gốc tăng lên, khả năng hệ thống xử lý nhiều người dùng hơn được cải thiện, nhưng sự cải thiện tốc độ tổng hợp chậm lại ở mật độ người dùng cao. Những kết quả này cung cấp những hiểu biết có giá trị cho việc thiết kế hệ thống đa người dùng với bộ ADC một bit, nhấn mạnh rằng việc tìm ra sự cân bằng hợp lý giữa số lượng người dùng và số lượng ăng-ten là rất cần thiết để đạt được hiệu suất tổng tốc độ truyền lên tối ưu.

Từ khóa - Hệ thống Đa Người Dùng, Bộ ADC Một Bit, Tốc độ tổng đường lên



Ngoc Phong Dao received his B.Sc. and Ph.D. degrees in Electronics and Telecommunications Engineering from the Hanoi University of Science and Technology (HUST) and his M.Sc. degree in Information Systems from the University of Technology - Hanoi National University. He is currently a lecturer at the Posts and Telecommunications Institute of Technology. His research interests include machine learning and optimization problems.



Hung Ngoc Dang received the B.Sc., M.Sc., and Ph.D. degrees from the Post and Telecommunications Institute of Technology (PTIT), Hanoi, Vietnam. He is currently a member of the Faculty of Information Technology at PTIT.